



Deposited via The University of Sheffield.

White Rose Research Online URL for this paper:

<https://eprints.whiterose.ac.uk/id/eprint/104333/>

Version: Accepted Version

Article:

Gasson, E., DeConto, R. and Pollard, D. (2016) Modeling the oxygen isotope composition of the Antarctic ice sheet and its significance to Pliocene sea level. *Geology*. ISSN: 0091-7613

<https://doi.org/10.1130/G38104.1>

Reuse

Items deposited in White Rose Research Online are protected by copyright, with all rights reserved unless indicated otherwise. They may be downloaded and/or printed for private study, or other acts as permitted by national copyright laws. The publisher or other rights holders may allow further reproduction and re-use of the full text version. This is indicated by the licence information on the White Rose Research Online record for the item.

Takedown

If you consider content in White Rose Research Online to be in breach of UK law, please notify us by emailing eprints@whiterose.ac.uk including the URL of the record and the reason for the withdrawal request.

1 Modeling the oxygen isotope composition of the Antarctic
2 ice sheet and its significance to Pliocene sea level

3 Edward Gasson^{1,2}, Robert M. DeConto¹, and David Pollard³

4 ¹Department of Geosciences, University of Massachusetts, Amherst, Massachusetts,
5 01003, USA

6 ²Department of Geography, The University of Sheffield, Sheffield, S10 2TN, UK

7 ³Earth and Environmental Systems Institute, Pennsylvania State University, University
8 Park, Pennsylvania, 16802, USA

9

10 **ABSTRACT**

11 Recent estimates of global mean sea level based on the oxygen isotope
12 composition of mid-Pliocene benthic foraminifera vary from 9 to 21 m above present,
13 which has differing implications for the past stability of the Antarctic ice sheet during an
14 interval with atmospheric CO₂ comparable to present. Here we simulate the oxygen
15 isotope composition of the Antarctic ice sheet for a range of configurations using isotope-
16 enabled climate and ice sheet models. We identify which ice-sheet configurations are
17 consistent with the oxygen isotope record and suggest a maximum contribution from
18 Antarctica to the mid-Pliocene sea level highstand of ~13 m. We also highlight that the
19 relationship between the oxygen isotope record and sea level is not constant when ice is
20 lost from deep marine basins, which has important implications for the use of oxygen
21 isotopes as a sea level proxy.

22

23 INTRODUCTION

24 There is significant interest in constraining the mid-Pliocene warm period
25 (MPWP) sea level highstand as it provides an opportunity to determine the magnitude of
26 maximum ice-sheet retreat during an interval with atmospheric CO₂ comparable to
27 present day (Raymo et al., 2009; Balco, 2015; Martínez-Botí et al., 2015). The MPWP
28 has also been used to evaluate climate and ice sheet model performance (e.g., De Boer et
29 al., 2015; DeConto and Pollard, 2016; Haywood et al., 2016), however these efforts have
30 been limited by poorly constrained sea-level estimates (Raymo et al., 2011).
31 Paleoshorelines can be used to reconstruct local relative sea level, however interpreting a
32 global eustatic signal from these records is complicated by glacio-isostatic adjustment,
33 dynamic topography, and vertical tectonics (Moucha et al., 2008; Raymo et al., 2011;
34 Rovere et al., 2014). Efforts to correct for dynamic topography using models currently
35 have large uncertainties (Dutton et al., 2015).

36 Alternative approaches to estimating past sea level make use of the change in the
37 oxygen isotope composition of benthic foraminifera relative to present values
38 ($\Delta\delta^{18}\text{O}_{\text{benthic}}$) and either independent estimates of deep-sea temperature (Dwyer and
39 Chandler, 2009) or simple assumptions based on the partitioning of $\Delta\delta^{18}\text{O}_{\text{benthic}}$ between
40 ice volume ($\Delta\delta^{18}\text{O}_{\text{seawater}}$) and temperature components ($\Delta\delta^{18}\text{O}_{\text{temperature}}$) (Miller et al.,
41 2012). The definition of $\Delta\delta^{18}\text{O}_{\text{benthic}}$ for the MPWP is important and will impact sea level
42 estimates based on this approach. $\Delta\delta^{18}\text{O}_{\text{benthic}}$ is variously cited as either 0.3‰ (e.g.,
43 Miller et al., 2012; Winnick and Caves, 2015) or 0.4‰ (e.g., Dutton et al., 2015),
44 depending on whether the differences are for Modern:MPWP (0.3‰) or
45 Holocene:MPWP (0.4‰), where the MPWP is the interglacial MIS G17 and $\delta^{18}\text{O}_{\text{benthic}}$ is

46 from the multi-site stack of Lisiecki and Raymo (2005). There are additional
47 uncertainties from analytical error in measuring $\delta^{18}\text{O}_{\text{benthic}}$ and potential hydrographic
48 effects (e.g. Dutton et al., 2015; Woodard et al., 2014; see Data Repository for more
49 discussion on calculation of $\Delta\delta^{18}\text{O}_{\text{benthic}}$).

50 In addition to changes in deep-sea temperature and ice mass, a number of recent
51 studies have also considered how changes in the mean oxygen isotope composition of the
52 ice sheets ($\delta^{18}\text{O}_{\text{ice}}$) may affect interpretation of $\Delta\delta^{18}\text{O}_{\text{benthic}}$ (Langebroek et al., 2010;
53 Winnick and Caves, 2015; Gasson et al., 2016). Changes in $\delta^{18}\text{O}_{\text{ice}}$ may be expected due
54 to changes in surface climate, with mean $\delta^{18}\text{O}_{\text{ice}}$ typically increasing in warmer climates
55 (Langebroek et al., 2010). Studies which have considered changes in $\delta^{18}\text{O}_{\text{ice}}$ include those
56 which have simulated changes in $\delta^{18}\text{O}$ of precipitation ($\delta^{18}\text{O}_{\text{precip.}}$) falling on the ice sheet
57 surface which is then tracked within the ice sheet based on internal ice velocities to
58 determine the mean oxygen isotopic composition of the ice sheet (DeConto et al., 2008;
59 Langebroek et al., 2010; Wilson et al., 2013; Gasson et al., 2016) and a novel isotope
60 mass-balance approach that estimated changes in $\delta^{18}\text{O}_{\text{ice}}$ based on modern $\delta^{18}\text{O}_{\text{precip.}}$ to
61 surface temperature relationships (Winnick and Caves, 2015). Here we follow the former
62 approach and calculate $\delta^{18}\text{O}_{\text{ice}}$ for a range of proposed MPWP Antarctic ice sheet
63 configurations (Pollard and DeConto, 2009; Mengel and Levermann, 2014; Austermann
64 et al., 2015; Pollard et al., 2015; DeConto and Pollard, 2016; Dowsett et al., 2016) and
65 ultimately calculate the Antarctic contribution to $\Delta\delta^{18}\text{O}_{\text{benthic}}$. This approach captures the
66 relative influences of climate and ice sheet geometry on its isotope composition, and has
67 the added advantage of quantifying the relative contributions of marine-based ice lying
68 above and below sea-level, to both global mean sea-level and $\delta^{18}\text{O}_{\text{seawater}}$.

69 **Pliocene Antarctic ice sheet simulations**

70 Previous simulations of the Antarctic ice sheets during the MPWP have shown
71 various stages of ice sheet retreat compared with modern – some of these simulations are
72 included in Table 1 and Figure DR1. These range from configurations with a collapsed
73 West Antarctic ice sheet and limited retreat of the East Antarctic ice sheet (e.g., Pollard
74 and DeConto, 2009; De Boer et al., 2015) to those with retreat deep into the East
75 Antarctic subglacial basins (e.g., Hill et al., 2007; Dolan et al., 2011; Pollard et al., 2015)
76 and various states in-between (e.g., Mengel and Levermann, 2014; Austermann et al.,
77 2015). The contribution to MPWP sea-level rise from the various Antarctic ice sheets
78 shown in Table 1 ranges from 3.7 to 17.8 m. Although these configurations can be
79 compared with sea level estimates and ice proximal evidence, they have not been
80 assessed in terms of compatibility with the $\delta^{18}\text{O}_{\text{benthic}}$ record. Here we repeat or
81 approximate these simulations using an oxygen isotope enabled climate and ice sheet
82 model (Mathieu et al., 2002; Wilson et al., 2013) to determine the Antarctic ice sheet
83 contribution to $\Delta\delta^{18}\text{O}_{\text{benthic}}$. The climate model used to calculate $\delta^{18}\text{O}_{\text{precip}}$ is setup as per
84 DeConto et al., (2012) for all simulations, with modifications to the Antarctic ice sheet
85 topography and extent.

86 The magnitude of $\Delta\delta^{18}\text{O}_{\text{benthic}}$ that can be attributed to changes in Antarctic ice-
87 sheet mass varies depending on assumptions about the ratio of $\Delta\delta^{18}\text{O}_{\text{seawater}}:\Delta\delta^{18}\text{O}_{\text{temperature}}$
88 and retreat of the Greenland ice sheet during the MPWP. Here we calculate an Antarctic
89 contribution to $\Delta\delta^{18}\text{O}_{\text{benthic}}$ of $0.18 \pm 0.13 \text{ ‰}$ (2σ). This is calculated using Monte Carlo
90 error propagation (e.g. Anderson, 1976) and follows previous assumptions for the
91 $\Delta\delta^{18}\text{O}_{\text{seawater}}:\Delta\delta^{18}\text{O}_{\text{temperature}}$ ratio (50:50 to 80:20), retreat of the Greenland ice sheet

92 during the MPWP (50 – 100 %) (Miller et al., 2012; Winnick and Caves, 2015) and also
93 considering different magnitudes of $\Delta\delta^{18}\text{O}_{\text{benthic}}$ (0.3–0.4 ‰). We apply an additional
94 uncertainty of ± 0.1 ‰ to $\Delta\delta^{18}\text{O}_{\text{benthic}}$ to account for analytical errors in measuring $\delta^{18}\text{O}$ of
95 benthic foraminifera. Note that assuming a larger $\Delta\delta^{18}\text{O}_{\text{benthic}}$ of 0.4‰ and following the
96 isotope mass-balance approach of Winnick and Caves (2015) we calculate a total
97 Antarctic (East and West Antarctic ice sheets) contribution to MPWP sea level of 8–12 m
98 (3–8 m assuming $\Delta\delta^{18}\text{O}_{\text{benthic}}$ of 0.3‰) with a total MPWP sea level rise of 13–18 m¹.

99 RESULTS AND DISCUSSION

100 Our calculations assume that each ice-sheet state in Table 1 and its internal $\delta^{18}\text{O}$
101 distribution has fully equilibrated with the corresponding steady-state climate. The $\delta^{18}\text{O}$
102 at each internal point within the ice is determined by Lagrangian tracing of steady-state
103 velocities back to the surface and assigning the $\delta^{18}\text{O}$ to that of $\delta^{18}\text{O}_{\text{precip}}$ at the surface
104 location. The $\delta^{18}\text{O}_{\text{precip}}$ values are taken from a corresponding GCM simulation. The $\delta^{18}\text{O}$
105 values are then integrated over the whole ice sheet to obtain the average $\delta^{18}\text{O}_{\text{ice}}$ values
106 (Wilson et al., 2013). We do the same for our pre-industrial control climate and ice sheet.
107 The $\Delta\delta^{18}\text{O}_{\text{ice}}$ values in Table 1 are the differences from this control. We then calculate
108 $\Delta\delta^{18}\text{O}_{\text{seawater}}$ following a mass-balance approach similar to that of Winnick and Caves
109 (2015); see Data Repository for equations.

¹ Assuming a $\Delta\delta^{18}\text{O}_{\text{seawater}}:\Delta\delta^{18}\text{O}_{\text{temperature}}$ ratio of 67:33 and a 1–4‰ increase in mean $\delta^{18}\text{O}_{\text{ice}}$, as per Winnick and Caves (2015) scenarios 1 and 2.

110 As a result of changes in surface climate, our MPWP GCM simulations show an
111 increase in mean $\delta^{18}\text{O}_{\text{precip}}$ falling over the Antarctic ice sheet of 6.0–7.5‰. However this
112 does not lead to an equivalent change in mean $\delta^{18}\text{O}_{\text{ice}}$, which has a smaller increase of
113 between 2.7 and 3.9‰ in our ice sheet simulations. This is due to changes in ice sheet
114 geometry and ice flow (see Figure 1). As the MPWP ice sheet retreats inland and away
115 from the ocean it retreats into regions that have lower $\delta^{18}\text{O}_{\text{precip}}$ values. Additionally, the
116 ice lost in warm climate simulations is often the isotopically heavier ice from the ice
117 margins as illustrated by comparing the simulated $\Delta\delta^{18}\text{O}_{\text{ice}}$ and $\Delta\delta^{18}\text{O}_{\text{precip}}$ values for
118 Austermann et al., (2015) with PRISM4 in Table 1. Therefore in MPWP simulations, if
119 there is no change in $\delta^{18}\text{O}_{\text{precip}}$ the Antarctic ice sheet would become isotopically lighter
120 (a decrease in $\delta^{18}\text{O}_{\text{ice}}$), rather than heavier. These effects should be considered when
121 using the modern relationship between surface temperature and $\delta^{18}\text{O}_{\text{precip}}$ to infer changes
122 in $\delta^{18}\text{O}_{\text{ice}}$ with changing surface climate (Winnick and Caves, 2015).

123 We next calculate how much the simulated MPWP Antarctic ice sheets would
124 alter $\delta^{18}\text{O}_{\text{seawater}}$ and hence the proportion of $\Delta\delta^{18}\text{O}_{\text{benthic}}$ that can be attributed to changes
125 in Antarctic ice mass. The calculated Antarctic contribution to $\delta^{18}\text{O}_{\text{seawater}}$ varies across
126 simulations from 0.16 to 0.39‰ because of differences in ice mass and changing mean
127 $\delta^{18}\text{O}_{\text{ice}}$. All of the simulated MPWP Antarctic ice sheets are within the expected range of
128 the $\delta^{18}\text{O}_{\text{benthic}}$ record ($0.18 \pm 0.13\text{‰}$), with the exception of the simulation of Pollard et al.
129 (2015), which has greater retreat than can be inferred from the $\delta^{18}\text{O}_{\text{benthic}}$ record based on
130 our prior assumptions. This is in part because of a 3.9‰ increase of mean $\delta^{18}\text{O}_{\text{ice}}$ for the
131 Pollard et al. (2015) ice sheet in the warm climate of the MPWP, however even with no

132 change in $\delta^{18}\text{O}_{\text{ice}}$, the $\delta^{18}\text{O}_{\text{seawater}}$ contribution (0.35‰) is still outside the range of the
133 $\delta^{18}\text{O}_{\text{benthic}}$ record.

134 These simulations have a sea level range of 3.7–17.8 m, highlighting that the
135 often-used calibration of $\delta^{18}\text{O}_{\text{seawater}}$ 0.01‰ per m of sea level change is not appropriate
136 for Antarctica (Figure 2; Miller et al., 2012; Winnick and Caves, 2015). This is in part
137 due to the generally lighter values of mean $\delta^{18}\text{O}_{\text{ice}}$ for the Antarctic ice sheet compared
138 with Northern Hemisphere ice sheets and because of changes in $\delta^{18}\text{O}_{\text{ice}}$ with changing
139 climate (Winnick and Caves, 2015). However another difference between $\delta^{18}\text{O}_{\text{seawater}}$ and
140 sea level records occurs when there is ice loss from subglacial basins. The sea level
141 change calculated here takes into account the infilling with seawater of subglacial basins
142 once they have been evacuated of ice. However $\delta^{18}\text{O}_{\text{seawater}}$ is a total ice mass signal and
143 this effect is not relevant to $\delta^{18}\text{O}_{\text{seawater}}$. There is therefore a decoupling between
144 $\delta^{18}\text{O}_{\text{seawater}}$ and sea level when there is significant change in marine based ice sheets, such
145 as the West Antarctic and large portions of the East Antarctic Ice Sheet. When ice is lost
146 from marine basins there will be a larger change in $\delta^{18}\text{O}_{\text{seawater}}$ than expected for the
147 equivalent change in sea level (see Figure 2). Note that this effect is accounted for by
148 Winnick and Caves (2015) for the Antarctic ice sheet on average, but that study does not
149 account for geographical locations of ice loss, which means that this effect is more
150 pronounced here (see Figure DR2). Repeating our isotope mass-balance calculations with
151 our simulated range for $\Delta\delta^{18}\text{O}_{\text{ice}}$ and accounting for the nonlinear relationship between
152 ice sheet mass change and sea level we calculate a total range for the Antarctic
153 contribution to MPWP sea level of -1 to 13 m (see Data Repository).

154 The nonlinear relationship between $\delta^{18}\text{O}_{\text{seawater}}$ and sea level partially causes the
155 large $\delta^{18}\text{O}_{\text{seawater}}$ contribution for the Pollard et al. (2015) Antarctic ice sheet, which has
156 significant loss of ice from deep subglacial basins, such as the Aurora and Wilkes
157 subglacial basins. A number of the other MPWP ice sheet simulations have partial retreat
158 into the East Antarctic subglacial basins, in particular the Wilkes Subglacial Basin
159 (Mengel and Levermann, 2014; Austermann et al., 2015; DeConto and Pollard, 2016).
160 Retreat into the Wilkes Subglacial Basin during the MPWP is also supported by a
161 sediment provenance study (Cook et al., 2013). The simulations with retreat into the
162 Wilkes but not the Aurora Subglacial Basin are within the expected range of the
163 $\delta^{18}\text{O}_{\text{benthic}}$ record. It can therefore be inferred that the constraints provided by the
164 $\delta^{18}\text{O}_{\text{benthic}}$ record indicates that there was not complete retreat into all of the deep
165 Antarctic subglacial basins during the MPWP. It should be noted that our simulations
166 account for increased precipitation in the continental interior under a warmer MPWP
167 climate. This increased precipitation generates interior ice sheet thickening that offsets
168 some of the ice lost from subglacial basins (Yamane et al., 2015).

169 **CONCLUSIONS AND IMPLICATIONS**

170 A recent reinterpretation of the $\delta^{18}\text{O}_{\text{benthic}}$ record suggested that there was
171 negligible mass loss from the East Antarctic ice sheet during the MPWP (Winnick and
172 Caves, 2015). Our results do not exclude this scenario; indeed the simulations that have a
173 collapsed West Antarctic but stable East Antarctic ice sheet (Pollard and DeConto, 2009;
174 De Boer et al., 2015) are within the uncertainty of the $\delta^{18}\text{O}_{\text{benthic}}$ record – as is the
175 possibility of a small negative (-1 m) Antarctic contribution to MPWP sea level.
176 However, these simulations are not consistent with other geological evidence for retreat

177 of portions of the East Antarctic ice sheet during the MPWP (Cook et al., 2013). A fuller
178 consideration of the uncertainties in the $\delta^{18}\text{O}_{\text{benthic}}$ record, in particular in calculations of
179 $\Delta\delta^{18}\text{O}_{\text{benthic}}$, does allow for greater mass loss from Antarctica during the MPWP.
180 Ultimately, the $\delta^{18}\text{O}_{\text{benthic}}$ record cannot exclude the possibility of large-scale retreat of
181 the Antarctic ice sheet during the mid-Pliocene warm period, but it does imply that the
182 Antarctic ice sheet contribution to sea level rise was at most ~ 13 m.

183

184 **SUPPLEMENTARY INFORMATION**

185 Isotope budget calculations:

186 Calculations shown in Table 1 follow the mass-balance approach used by
187 Winnick and Caves (2015):

$$188 \quad M_{\text{O}} + M_{\text{GIS}} + M_{\text{WAIS}} + M_{\text{EAIS}} = M_{\text{pO}} + M_{\text{pGIS}} + M_{\text{pWAIS}} + M_{\text{pEAIS}}$$

189 (1)

$$190 \quad M_{\text{O}}\delta^{18}\text{O}_{\text{SW}} + M_{\text{GIS}}\delta^{18}\text{O}_{\text{GIS}} + M_{\text{WAIS}}\delta^{18}\text{O}_{\text{WAIS}} + M_{\text{EAIS}}\delta^{18}\text{O}_{\text{EAIS}} = \\ M_{\text{pO}}\delta^{18}\text{O}_{\text{pSW}} + M_{\text{pGIS}}\delta^{18}\text{O}_{\text{pGIS}} + M_{\text{pWAIS}}\delta^{18}\text{O}_{\text{pWAIS}} + M_{\text{pEAIS}}\delta^{18}\text{O}_{\text{pEAIS}}$$

191 (2)

192 Where M_x is the total mass of the modern (M_{O}) and Pliocene (M_{pO}) oceans and Greenland
193 (GIS), West Antarctic (WAIS) and East Antarctic (EAIS) ice sheets. Winnick and Caves
194 (2015) solved these equations for M_{pO} and M_{pEAIS} . In this study we are interested in the
195 Antarctic contribution to $\Delta\delta^{18}\text{O}_{\text{seawater}}$ and are using Pliocene Antarctic ice sheet model
196 simulations for M_{pEAIS} . We therefore ignore changes in the Greenland ice sheet and treat
197 the West and East Antarctic ice sheets together:

198 $M_O + M_{AIS} = M_{pO} + M_{pAIS}$ (3)

199 $M_O \delta^{18}O_{SW} + M_{AIS} \delta^{18}O_{AIS} = M_{pO} \delta^{18}O_{pSW} + M_{pAIS} \delta^{18}O_{pAIS}$ (4)

200 We take M_{pAIS} and $\delta^{18}O_{pAIS}$ from our simulations and then calculate $\delta^{18}O_{pSW}$ (the
201 Antarctic contribution to $\Delta\delta^{18}O_{benthic}$):

202
$$\delta^{18}O_{pSW} = \frac{M_O \delta^{18}O_{SW} + M_{AIS} \delta^{18}O_{AIS} - M_{pAIS} \delta^{18}O_{pAIS}}{M_O + M_{AIS} - M_{pAIS}}$$
 (5)

203 Our simulated value for the modern mean oxygen isotopic composition of the Antarctic
204 ice sheet is -33.8‰ . This is considerably higher than the calculated whole Antarctic
205 value of -54.7‰ of Lhomme et al. (2005). The reason for this discrepancy is due in part
206 to a GCM bias of $\sim 10\text{‰}$ in modern values for $\delta^{18}O_{precip.}$ when compared with
207 observations over the Antarctic interior, caused by modeled surface temperatures that are
208 too warm (Mathieu et al., 2002). Additionally, our values are in equilibrium with the
209 modern surface climate, in contrast to the values from Lhomme et al. (2005) which
210 account for change in $\delta^{18}O_{ice}$ through successive glacial periods with predominantly
211 lower $\delta^{18}O_{precip.}$ We therefore use the Lhomme et al. (2005) values (-54.7‰) throughout
212 for modern $\delta^{18}O_{AIS}$. For Pliocene values of $\delta^{18}O_{pAIS}$ we use the anomaly between our
213 Pliocene ($\delta^{18}O_{PLIOCENE}$) and pre-industrial control ($\delta^{18}O_{CONTROL}$) simulations:

214
$$\delta^{18}O_{pAIS} = -54.7 + (\delta^{18}O_{PLIOCENE} - \delta^{18}O_{CONTROL})$$
 (6)

215 Note that we do not change mean ocean $\delta^{18}O$ in our GCM simulations. The GCM
216 used is an isotope-enabled version of the GENESIS GCM.

217

218 Calculation of $\Delta\delta^{18}\text{O}_{\text{benthic}}$:

219 In the main paper we highlight two different values for $\Delta\delta^{18}\text{O}_{\text{benthic}}$ in the
220 literature, 0.31‰ for Modern:G17 and 0.40‰ for Holocene:G17. Although we do
221 not suggest a preference for either value, here we discuss reasons for these
222 differences. The modern value for $\delta^{18}\text{O}_{\text{benthic}}$ in the LR04 stack (Lisiecki and
223 Raymo, 2005) is 3.23‰, compared with 3.32‰ when averaged over the last 10
224 kyr and 2.92‰ during MIS G17 (2.95 Ma). The higher value for Holocene
225 $\delta^{18}\text{O}_{\text{benthic}}$ may be a result of the ice sheets having lower mean $\delta^{18}\text{O}_{\text{ice}}$ as they
226 would be less equilibrated to modern $\delta^{18}\text{O}_{\text{precip.}}$. Additionally, remnant glacial ice
227 in the early Holocene would also lead to higher values for $\delta^{18}\text{O}_{\text{benthic}}$ when
228 averaged over the last 10 kyr. Both of these arguments would suggest that
229 Modern:MPWP should be used for $\Delta\delta^{18}\text{O}_{\text{benthic}}$ over Holocene:MPWP. However,
230 these effects could also lead to higher $\delta^{18}\text{O}_{\text{benthic}}$ during MPWP interglacials,
231 which are time-averaged due to poor temporal resolution (2.5–5 kyr). A potential
232 solution would be to use a high-resolution $\delta^{18}\text{O}_{\text{benthic}}$ record. The recently
233 published deep-Pacific ODP Site 1208 shows a Modern:MPWP $\Delta\delta^{18}\text{O}_{\text{benthic}}$ of
234 0.49‰ (Woodard et al., 2015). However individual sites may also be affected by
235 ocean circulation changes (this could equally affect the LR04 stack which is
236 weighted towards the Atlantic). Indeed other high-resolution sites show a
237 Modern:MPWP $\Delta\delta^{18}\text{O}_{\text{benthic}} < 0.3\text{‰}$ (M. Patterson, personal communication). A
238 more detailed statistical analysis of $\Delta\delta^{18}\text{O}_{\text{benthic}}$ is required for individual sites
239 (e.g. Mudelsee et al., 2014), which is beyond the scope of this paper. Here we use

240 the range of 0.3–0.4‰ for $\Delta\delta^{18}\text{O}_{\text{benthic}}$ and add a $\pm 0.1\%$ uncertainty for analytical
241 error, giving a total range of 0.2–0.5‰.

242

243 Calculation of Antarctic contribution to MPWP sea level:

244 We calculate maximum and minimum contributions from the Antarctic ice sheets to
245 MPWP sea level. From $\Delta\delta^{18}\text{O}_{\text{benthic}}$ we calculate an Antarctic ice sheet component of 0.18
246 ± 0.13 ‰ using Monte-Carlo error propagation to account for uncertainty in the
247 $\Delta\delta^{18}\text{O}_{\text{seawater}}:\Delta\delta^{18}\text{O}_{\text{temperature}}$ ratio, retreat of the Greenland ice sheet and analytical error in
248 $\delta^{18}\text{O}_{\text{benthic}}$. Rearranging equation (5) we determine the Antarctic ice sheet mass change
249 required for $\Delta\delta^{18}\text{O}_{\text{seawater}}$ at the upper (0.31‰) and lower ends (0.05‰) of our error
250 estimate. For $\Delta\delta^{18}\text{O}_{\text{ice}}$ we use the upper and lower estimates from our simulations (+2.7 to
251 +3.9‰). This results in an Antarctic mass change of +0.53 to -6.61×10^{18} kg. To account
252 for the nonlinear relationship between ice sheet mass change and sea level due to the
253 effect of marine-subglacial basins we use the calibration generated from an Antarctic ice
254 sheet deglaciation simulation (Figure DR2) to convert from mass change to sea level
255 change. This leads to a lower estimate for the Antarctic contribution to MPWP sea level
256 of -1.4 m (a sea level fall) and an upper estimate of +13.1 m.

257 **ACKNOWLEDGMENTS**

258 We thank Ken Miller, Matthew Winnick and one anonymous reviewer for their
259 constructive comments and suggestions. We also thank Molly Patterson, Ben Keisling
260 and Kate Hibbert for discussions that helped improve the manuscript. This study was
261 supported by US National Science Foundation awards OCE-1202632 (“PLIOMAX”) and
262 AGS-1203910.

263 **REFERENCES CITED**

- 264 Anderson, G.M., 1976, Error propagation by the Monte Carlo method in geochemical
265 calculations: *Geochimica et Cosmochimica Acta*, v. 40, no. 12, p. 1533–1538.
- 266 Austermann, J., Pollard, D., Mitrovica, J.X., Moucha, R., Forte, A.M., DeConto, R.M.,
267 Rowley, D.B., and Raymo, M.E., 2015, The impact of dynamic topography change
268 on Antarctic ice sheet stability during the mid-Pliocene warm period: *Geology*, v. 43,
269 p. 927–930, doi:10.1130/G36988.1.
- 270 Balco, G., 2015, The absence of evidence of absence of the East Antarctic Ice Sheet:
271 *Geology*, v. 43, p. 943–944, doi:10.1130/focus102015.1.
- 272 Cook, C.P., et al., 2013, Dynamic behaviour of the East Antarctic ice sheet during
273 Pliocene warmth: *Nature Geoscience*, v. 6, p. 765–769, doi:10.1038/ngeo1889.
- 274 De Boer, B., et al., 2015, Simulating the Antarctic ice sheet in the late-Pliocene warm
275 period: PLISMIP-ANT, an ice-sheet model intercomparison project: *The*
276 *Cryosphere*, v. 9, no. 3, p. 881–903, doi:10.5194/tc-9-881-2015.
- 277 DeConto, R.M., and Pollard, D., 2016, Contribution of Antarctica to past and future sea-
278 level rise: *Nature*, v. 531, p. 591–597, doi:10.1038/nature17145.
- 279 DeConto, R.M., Pollard, D., Wilson, P.A., Pälike, H., Lear, C.H., Pagani, M., 2008,
280 Thresholds for Cenozoic bipolar glaciation: *Nature*, v. 455, p.652–656,
281 doi:10.1038/nature07337
- 282 DeConto R.M., Pollard, D., Kowalewski, D., 2012, Modeling Antarctic ice sheet and
283 climate variations during Marine Isotope Stage 31: *Global and Planetary Change*, v.
284 88, p 45–52, doi:10.1016/j.glopacha.2012.03.003

- 285 Dolan, A.M., Haywood, A.M., Hill, D.J., Dowsett, H.J., Hunter, S.J., Lunt, D.J., and
286 Pickering, S.J., 2011, Sensitivity of Pliocene ice sheets to orbital forcing:
287 Palaeogeography, Palaeoclimatology, Palaeoecology, v. 309, p. 98–110,
288 doi:10.1016/j.palaeo.2011.03.030.
- 289 Dowsett, H., Dolan, A., Rowley, D., Pound, M., Salzmann, U., Robinson, M., Chandler,
290 M., Foley, K., and Haywood, A., 2016, The PRISM4 (mid-Piacenzian)
291 palaeoenvironmental reconstruction: *Climate of the Past Discussions*, v. 4, p. 1–39,
292 doi:10.5194/cp-2016-33.
- 293 Dutton, A., Carlson, A.E., Long, A.J., Milne, G.A., Clark, P.U., DeConto, R., Horton,
294 B.P., Rahmstorf, S., and Raymo, M.E., 2015, Sea-level rise due to polar ice-sheet
295 mass loss during past warm periods: *Science*, v. 349, doi:10.1126/science.aaa4019.
- 296 Dwyer, G.S., and Chandler, M.A., 2009, Mid-Pliocene sea level and continental ice
297 volume based on coupled benthic Mg/Ca palaeotemperatures and oxygen isotopes:
298 *Philosophical transactions. Series A, Mathematical, physical, and engineering*
299 *sciences*, v. 367, no. p. 157–168, doi:10.1098/rsta.2008.0222.
- 300 Gasson, E., DeConto, R.M., Pollard, D., and Levy, R.H., 2016, Dynamic Antarctic ice
301 sheet during the early to mid-Miocene: *Proceedings of the National Academy of*
302 *Sciences of the United States of America*, p. 201516130,
303 doi:10.1073/pnas.1516130113.
- 304 Haywood, A.M., Dowsett, H.J., and Dolan, A.M., 2016, Integrating geological archives
305 and climate models for the mid-Pliocene warm period: *Nature Communications*, v. 7,
306 doi:10.1038/ncomms10646.

- 307 Hill, D.J., Haywood, A.M., Hindmarsh, R.C.A., and Valdes, P.J., 2007, Characterizing
308 ice sheets during the Pliocene: Evidence from data and models, *in* Williams, M., and
309 Haywood, A.M., eds., *Deep-Time Perspectives on Climate Change: Marrying the*
310 *signal from Computer Models and Biological Proxies.*, p. 517–538.
- 311 Langebroek, P.M., Paul, A., and Schulz, M., 2010, Simulating the sea level imprint on
312 marine oxygen isotope records during the middle Miocene using an ice sheet–climate
313 model: *Paleoceanography*, v. 25, PA4203, doi:10.1029/2008PA001704.
- 314 Lhomme, N., Clarke, G.K.C., and Ritz, C., 2005, Global budget of water isotopes
315 inferred from polar ice sheets: *Geophysical Research Letters*, v. 32, L20502,
316 doi:10.1029/2005GL023774.
- 317 Lisiecki, L.E., and Raymo, M.E., 2005, A Pliocene-Pleistocene stack of 57 globally
318 distributed benthic $\delta^{18}\text{O}$ records: *Paleoceanography*, v. 20,
319 doi:10.1029/2004PA001071.
- 320 Martínez-Botí, M.A., Foster, G.L., Chalk, T.B., Rohling, E.J., Sexton, P.F., Lunt, D.J.,
321 Pancost, R.D., Badger, M.P.S., and Schmidt, D.N., 2015, Plio-Pleistocene climate
322 sensitivity evaluated using high-resolution CO₂ records: *Nature*, v. 518, p. 49–54,
323 doi:10.1038/nature14145.
- 324 Mathieu, R., Pollard, D., Cole, J.E., White, J.W.C., Webb, R.S., and Thompson, S.L.,
325 2002, Simulation of stable water isotope variations by the GENESIS GCM for
326 modern conditions: *Journal of Geophysical Research*, v. 107, p. 1–18,
327 doi:10.1029/2001JD900255.
- 328 Mengel, M., and Levermann, A., 2014, Ice plug prevents irreversible discharge from East
329 Antarctica: *Nature Climate Change*, v. 4, p. 451–455, doi:10.1038/nclimate2226.

- 330 Miller, K.G., Wright, J.D., Browning, J.V., Kulpecz, A., Kominz, M., Naish, T.R.,
331 Cramer, B.S., Rosenthal, Y., Peltier, W.R., and Sosdian, S., 2012, High tide of the
332 warm Pliocene: Implications of global sea level for Antarctic deglaciation: *Geology*,
333 v. 40, p. 407–410, doi:10.1130/G32869.1.
- 334 Moucha, R., Forte, A.M., Mitrovica, J.X., Rowley, D.B., Quéré, S., Simmons, N.a., and
335 Grand, S.P., 2008, Dynamic topography and long-term sea-level variations: There is
336 no such thing as a stable continental platform: *Earth and Planetary Science Letters*,
337 v. 271, p. 101–108, doi:10.1016/j.epsl.2008.03.056.
- 338 Mudelsee, M., Bickert, T., Lear, C.H., Lohmann, G., 2014, Cenozoic climate changes: A
339 review based on time series analysis of marine benthic $\delta^{18}\text{O}$ records: *Reviews of*
340 *Geophysics*, v. 52, no. 3, p. 333–374, doi:10.1002/2013RG000440
- 341 Pollard, D., and DeConto, R.M., 2009, Modelling West Antarctic ice sheet growth and
342 collapse through the past five million years: *Nature*, v. 458, p. 329–332,
343 doi:10.1038/nature07809.
- 344 Pollard, D., and DeConto, R.M., 2012, Description of a hybrid ice sheet-shelf model, and
345 application to Antarctica: *Geoscientific Model Development*, v. 5, p. 1273–1295,
346 doi:10.5194/gmd-5-1273-2012.
- 347 Pollard, D., DeConto, R.M., and Alley, R.B., 2015, Potential Antarctic Ice Sheet retreat
348 driven by hydrofracturing and ice cliff failure: *Earth and Planetary Science Letters*,
349 v. 412, p. 112–121, doi:10.1016/j.epsl.2014.12.035.
- 350 Raymo, M.E., Hearty, P., De Conto, R., O’Leary, M., Dowsett, H.J., Robinson, M.H.,
351 and Mitrovica, J.X., 2009, PLIOMAX: Pliocene maximum sea level project: *PAGES*
352 *News*, v. 17, p. 58–59.

- 353 Raymo, M.E., Mitrovica, J.X., O’Leary, M.J., DeConto, R.M., and Hearty, P.J., 2011,
354 Departures from eustasy in Pliocene sea-level records: *Nature Geoscience*, v. 4,
355 p. 328–332, doi:10.1038/ngeo1118.
- 356 Rovere, A., Raymo, M.E., Mitrovica, J.X., Hearty, P.J., O’Leary, M.J., and Inglis, J.D.,
357 2014, The Mid-Pliocene sea-level conundrum: Glacial isostasy, eustasy and dynamic
358 topography: *Earth and Planetary Science Letters*, v. 387, p. 27–33,
359 doi:10.1016/j.epsl.2013.10.030.
- 360 Wilson, D.S., Pollard, D., Deconto, R.M., Jamieson, S.S.R., and Luyendyk, B.P., 2013,
361 Initiation of the West Antarctic Ice Sheet and estimates of total Antarctic ice volume
362 in the earliest Oligocene: *Geophysical Research Letters*, v. 40, p. 4305–4309,
363 doi:10.1002/grl.50797.
- 364 Winnick, M.J., and Caves, J.K., 2015, Oxygen isotope mass-balance constraints on
365 Pliocene sea level and East Antarctic Ice Sheet stability: *Geology*, v. 43, p. 879–882,
366 doi:10.1130/G36999.1.
- 367 Woodard, S.C., Rosenthal, Y., Miller, K.G., Wright, J.D., Chiu, B.K., Lawrence, K.T.,
368 2014, Antarctic role in Northern Hemisphere glaciation: *Science*, v. 346, p. 847–851,
369 doi:10.1126/science.1255586.
- 370 Yamane, M., Yokoyama, Y., Abe-Ouchi, A., Obrochta, S., Saito, F., Moriwaki, K., and
371 Matsuzaki, H., 2015, Exposure age and ice-sheet model constraints on Pliocene East
372 Antarctic ice sheet dynamics: *Nature Communications*, v. 6,
373 doi:10.1038/ncomms8016.

374

375

376

377
 378
 379

TABLE 1. ANTARCTIC ICE SHEET CONTRIBUTION TO SEA LEVEL AND $\Delta\delta^{18}\text{O}_{\text{seawater}}$

Study	$\Delta\text{sea level}$ (m)	Δmass (10^{18} kg)	$\Delta\delta^{18}\text{O}_{\text{precip}}$ (‰)	$\Delta\delta^{18}\text{O}_{\text{ice}}$ (‰)	$\Delta\delta^{18}\text{O}_{\text{seawater}}$ (‰)	$\Delta\delta^{18}\text{O}_{\text{seawater}}$ (‰)
Pollard and DeConto, 2009*	3.7	-2.8	6.0	2.9	0.16	0.11 [#]
Mengel and Levermann, 2014 [†]	5.4	-3.6	6.4	3.6	0.20	0.14 [#]
Austermann et al., 2015*	8.8	-4.9	6.6	3.6	0.25	0.20 [#]
PRISM4 [§]	9.1	-5.0	6.6	2.7	0.24	0.20 [#]
DeConto and Pollard, 2016*	11.3	-6.1	7.5	3.8	0.29	0.25 [#]
Pollard et al., 2015*	17.8	-8.8	7.2	3.9	0.39	0.35 [#]

Note: Calculations assume a modern mean $\delta^{18}\text{O}_{\text{ice}}$ of -54.7‰ for the Antarctic ice sheet (Lhomme et al. 2005). Values for $\delta^{18}\text{O}_{\text{ice}}$ are equilibrium values following 300 kyr of simulation, shown relative to a pre-industrial control simulation

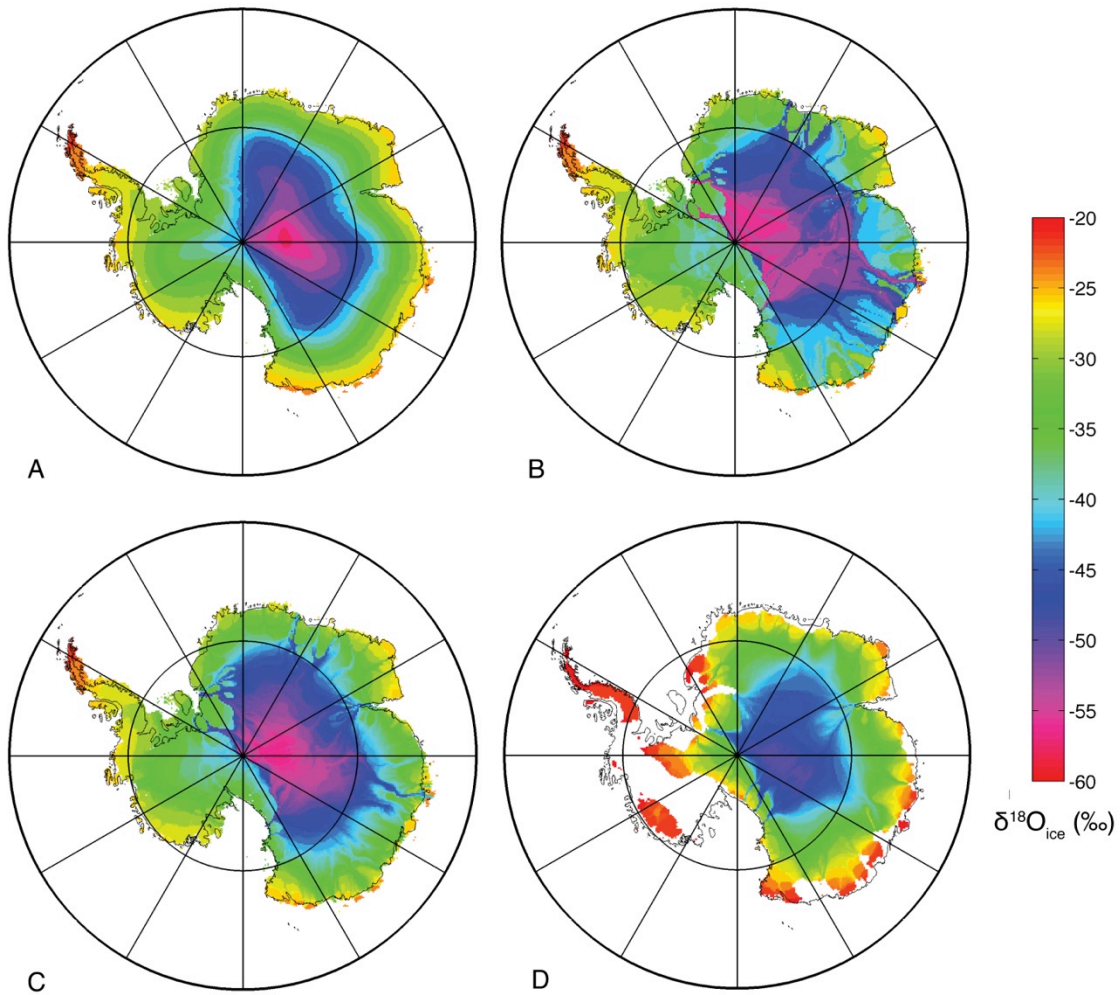
^{*}reproduced with addition of isotopes

[†]approximate whole ice sheet simulation, showing similar response to Wilkes Basin simulations of Mengel and Levermann (2014). This simulation is created by imposing high ocean melt rates (a factor of 10 increase in the value of K in Equation 17 of (Pollard and DeConto, 2012)) and uses the same ice sheet physics as the Pollard and DeConto (2009) simulation

[§]PRISM4 ice sheet is maintained by imposing a surface mass balance mask which prevents areal expansion of the ice sheet from its starting position, ice thicknesses are maintained by adjusting basal sliding coefficients

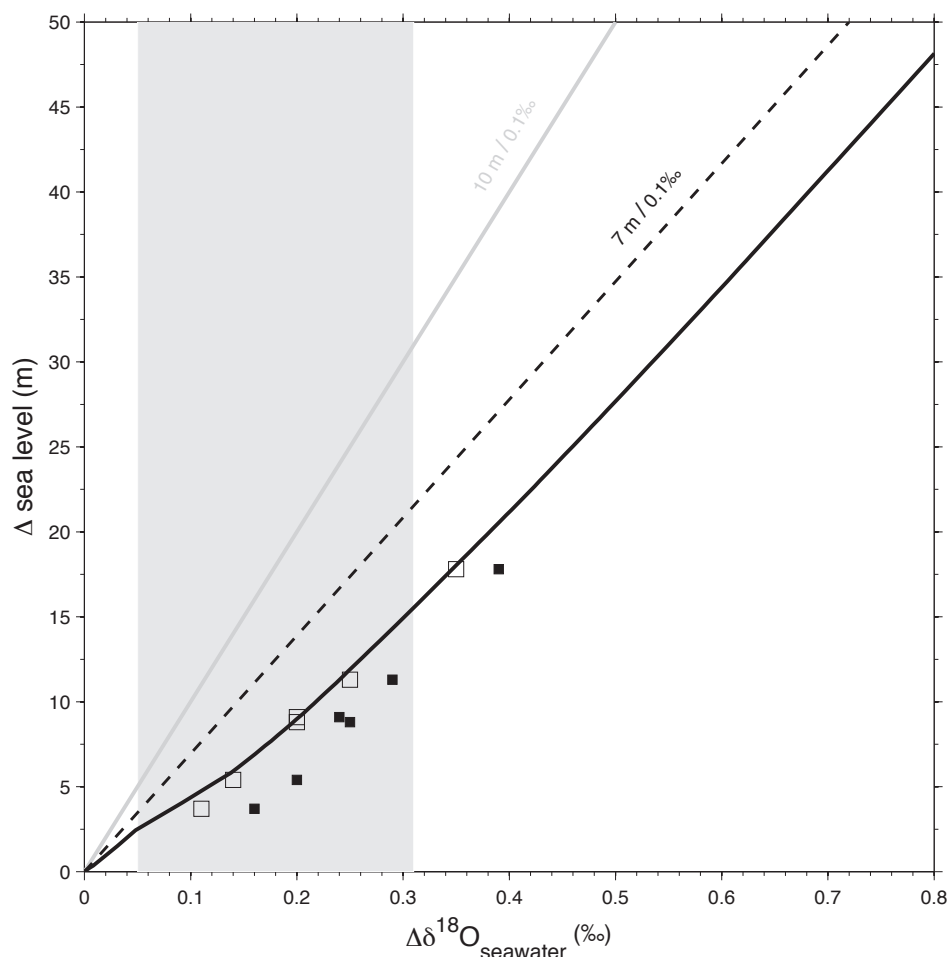
[#]no change in $\delta^{18}\text{O}_{\text{ice}}$, values fixed at modern

380
 381
 382
 383
 384
 385
 386
 387
 388



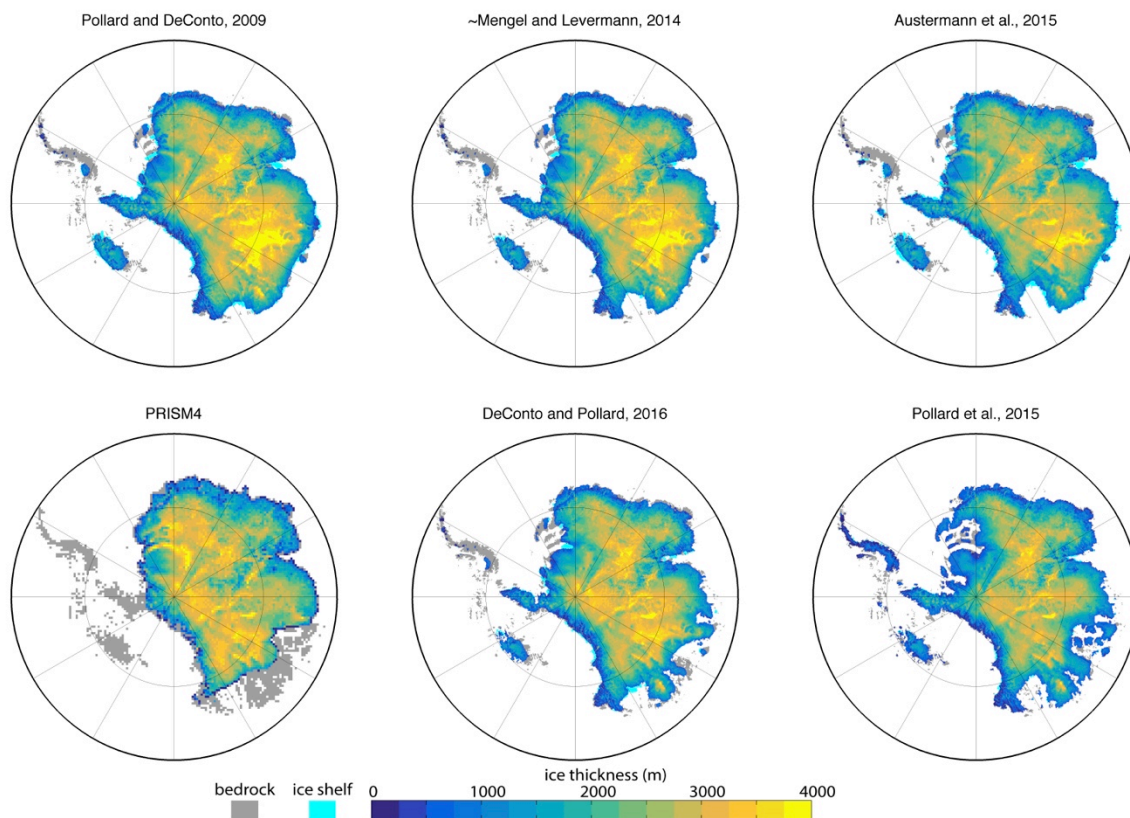
389
390 Figure 1. Simulated $\delta^{18}\text{O}_{\text{ice}}$ at different ice depths. A: Modern ice surface layer. B:
391 Modern ice basal layer. C: Modern depth averaged. D: Pliocene depth averaged
392 (DeConto and Pollard, 2016).

393
394
395
396
397



398
399 Figure 2. Relationship between $\delta^{18}\text{O}_{\text{seawater}}$ and sea level. Gray line shows the commonly
400 used 10 m / 0.1 ‰ calibration (e.g. Woodard et al., 2014). Black dashed line shows the
401 calibration for Antarctica for a mean $\delta^{18}\text{O}_{\text{ice}}$ of -54.7 ‰ (Lhomme et al., 2005), ignoring
402 the impact of marine-based ice on sea level. Black line is an Antarctic ice sheet deglacial
403 simulation, for a mean $\delta^{18}\text{O}_{\text{ice}}$ of -54.7 ‰, the change in gradient of the black line is
404 caused by the initial loss of marine-based ice. White and black squares are Antarctic ice
405 sheet simulations from Table 1, with fixed $\delta^{18}\text{O}_{\text{ice}}$ and changing $\delta^{18}\text{O}_{\text{ice}}$, respectively.
406 Gray band shows the Antarctic contribution to $\Delta\delta^{18}\text{O}_{\text{seawater}}$ (0.18 ± 0.13 ‰).

407



408

409

Figure DR1. Previously published Antarctic ice sheet simulations for the mid-Pliocene

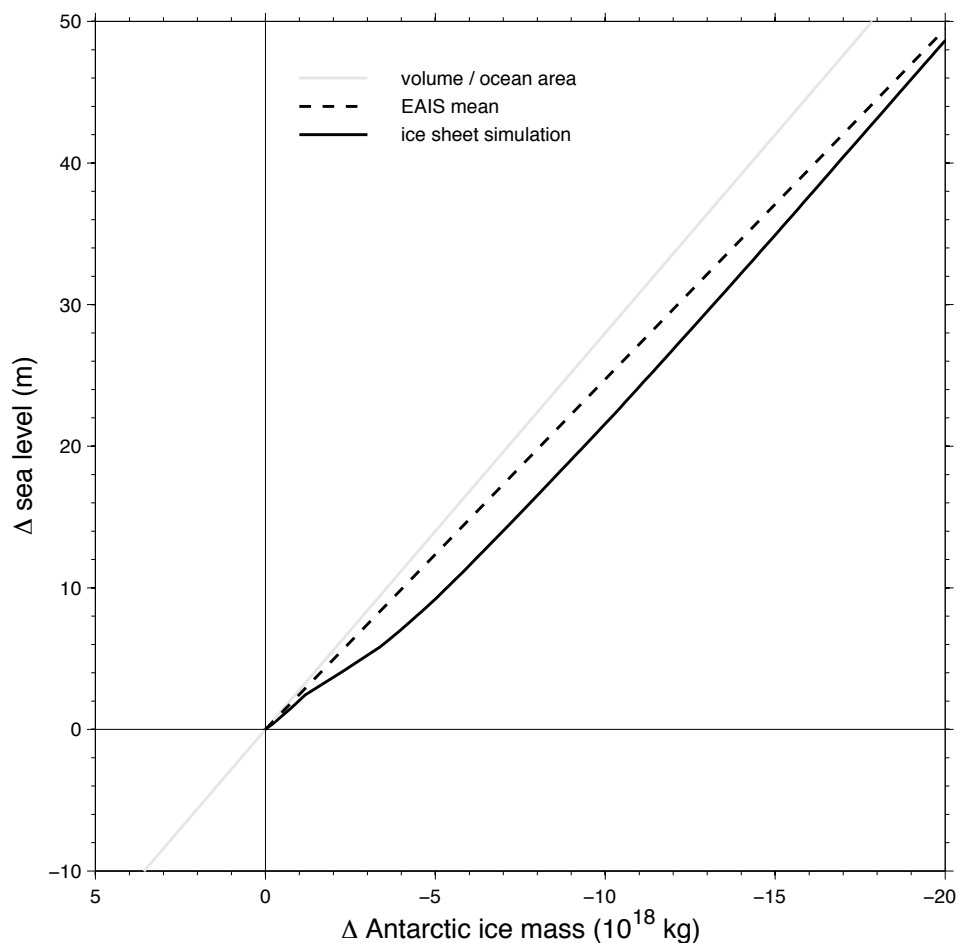
410

warm period, repeated or approximated here using isotope enabled climate and ice sheet

411

models.

412



413
414 Figure DR2. Relationship between Antarctic ice sheet mass change and sea level change.
415 Gray line shows ice volume divided by ocean area after accounting for the change in state
416 from ice to seawater. Dashed black line is the mean relationship for the East Antarctic ice
417 sheet for a total ice mass of 21.55×10^{18} kg and sea level rise of 53.3 m (Fretwell et al.,
418 2013; Winnick and Caves, 2015). Black line is from an Antarctic ice sheet deglacial
419 simulation with initial loss of ice predominantly from marine subglacial basins.
420